Solar radiation effects on the epoxy adhesive temperature used to bond CFRP to concrete road bridges

M. Breveglieri[1], B. Weber[1], C. Czaderski[1]
[1.] Empa - Swiss Federal Laboratories for Materials Science and Technology, Dübendorf, Switzerland

Introduction

Carbon Fiber Polymers are being frequently used to strengthened reinforced concrete (RC) structures, the advantages of employing this material lie in the high strength/weight ratio and resistance to corrosion. The latter property allows the application of this material on the external surface of the structural element, without any (or with limited) type of protection.
CFRP is typically bonded to the concrete surface by means of epoxy-based adhesives. When exposed to high temperatures, the adhesive softens and the bond between concrete and FRP is lost. The temperature at which the structural adhesive loses its mechanical strength is called the glass transition temperature. In the case of the commercially available structural adhesives for FRP applications, the glass transition temperature can be approximately estimated around 50-60°C [1].
This value might be considered relatively low if compared with the temperature that can be reached in the adhesive when civil structures, such as such as road bridges, are exposed to elevated ambient temperature and solar radiation.
In a recent project [2] focused on the strengthening of a lateral cantilever of hollow box bridge girder (Figure 1), experimental tests were performed to evaluate the maximum achievable temperature in the adhesive during mastic asphalt application and throughout the service-life of the structure. Figure 2 shows a long-term experimental set-up of a one-way slab strengthened with two CFRP strips under sustained load and exposed to the external environment. For the slab, shown in Figure 2, not any layer of asphalt was provided, and the CFRP was protected from humidity and UV rays by using only a layer of special gray color sealing paint. Tests showed that temperature achieved in the adhesive is approximately 50°C: a value comparable to the glass transition temperature. This outcome highlights a critical point in the CFRP-concrete bond for such type of applications. As a consequence of the changes of temperature in the cross-section of the slab, thermal stresses are generated.

This paper presents a preliminary study on the effects of high temperatures and direct exposure to solar radiation, on CFRP strips bonded to the top surface of one-way RC slabs.

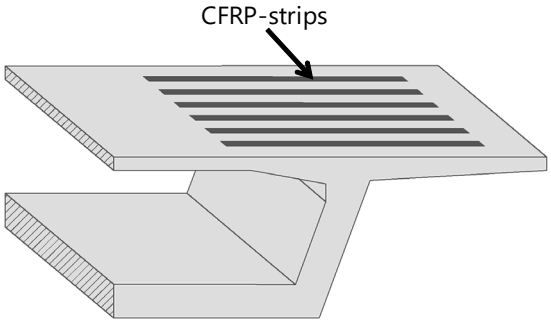

Figure 1. Half-cross section of a hollow box girder bridge. CFRP application for the strengthening of the lateral cantilever.

Figure 2. Long-term experimental set-up, simulating a CFRP strengthened lateral cantilever.

In this study, two modules of the COMSOL Multiphysics® software are used: the Heat Transfer and the Structural Mechanics modules. The Heat Transfer with Surface-to-Surface Radiation is used to consider the effects of the daily fluctuation of air temperature and the solar radiation on the temperature of the epoxy adhesive, whereas the Structural Mechanics module is used to evaluate the thermal stresses generated by temperature changes in the cross-section. This work compares two different modeling approaches. In the first, *full-domain approach*, the adhesive layer and the CFRP strips are modeled as solid elements; in the second, *lumped*

boundary approach, they are modeled using the "Thin Layer" approximation in the heat transfer problem and as a layered shell in the structural mechanic's problem. Since the CFRP strips and adhesive are characterized by thin geometry, modeling them through thin layers as a lumped boundary can make the meshing procedure easier and save computational time. For the concrete, a solid geometry is adopted in both cases.

Problem definition and governing equations

The object of this study is a CFRP strengthened RC one-way slab exposed to the external environment as shown in Figure 2. The slab (5 x 1 x 0.22 m^3) is strengthened with two 5-m-long CFRP strips of width and thickness, equal to 100 mm and 1.2 mm, respectively. The thickness of the adhesive layer can be approximated to 2 mm. The slab is supported at its center and restrained by bilateral support at one end. A sustained load of 14.8 kN is applied at the free end, nevertheless, as this is a preliminary study, gravity and sustained loads are not considered. The aim of this paper is to compare two different modeling strategies to calculate the temperature distribution along the cross-section with a particular focus on the temperature of the adhesive, and the thermal stress generated in the CFRP due to the daily temperature fluctuation and sun movement. A two-day simulation is performed, to asses the validity of the numerical models. It has to mention, that the application of CFRP strip on the top of the surface without an asphalt layer as protection is an unusual configuration and only for research purposes.

The proposed problem consists of a one way coupled transient thermo-mechanical problem. This means that the thermal problem is initially computed by solving Eq. (1) and subsequently, the obtained temperature filed (T) is used to solve the mechanical problem by solving Eq. (2). It differentiates from a fully coupled problem, where both Eq.1 and 2 are solver at the same time.

$$\rho C_P \frac{\partial T}{\partial t} + \nabla \mathrm{q} = 0, \qquad with\ q = -k\nabla T \tag{1}$$

$$\nabla \sigma = F_v \tag{2}$$

In Eq. (1), the first term represents the change of internal energy (ρ, is the density of the material and C_p, the heat capacity) and the second term, by means of the Fourier's law, serves to define the conductive heat flux q (k, is the thermal conductivity). The initial, Eq. (3) and boundary condition, Eq. (4) associated to Eq. (1) can be written as:

$$T = T_0 \tag{3}$$

$$-k\frac{\partial T}{\partial n} + q_c + q_r = 0 \tag{4}$$

Where T_0 is the initial temperature, meanwhile q_c and q_r as shown in Eqs. (5) and (6) stands for the heat transfer contribution at the boundary attributable to convention and radiation.

$$q_c = h(T_{ext} - T) \tag{5}$$

T_{ext} is the extremal temperature which is assumed to be varying during the day and h, represents the convection-heat transfer coefficient. In Eq. (6) shows the expression for a radiative boundary condition; two different wavelengths: solar (short-wave radiation λ_1<2.5μm) and ambient (long-wave radiation λ_2> 2.5μm) are considered[3].

$$q_r = \sum_{i=1}^{2} \varepsilon_{\lambda i}\left(G_{\lambda i} - e_{b,\lambda i}(T) \cdot FEP_{\lambda i}(T)\right) \tag{6}$$

For each i^{th} wavelength, in Eq. (6): $\varepsilon_{\lambda i}$ is the emissivity , $G_{\lambda i}$ is the incoming radiation, $e_{b,\lambda i}(T)$ is the power radiated according to the Stefan-Boltzmann law and $FEP_{\lambda i}(T)$ is the fractional emissive power. The incoming radiation $G_{\lambda i}$, is calculated taking into account both the solar $G_{\lambda i.ext}$ and the ambient irradiance, $G_{\lambda i,amb}$, as shown in Eq. (7):

$$G_{\lambda i} = G_{\lambda i,amb} + G_{\lambda i.ext} \tag{7}$$

The component $G_{\lambda i.amb}$ is calculated in a similar way as the le last term of Eq.6, where T needs to be assumed as the ambient temperature, T_{amb}. The solar irradiance, $G_{\lambda i.ext}$, is a function of the position of the sun expressed as the zenith angle θ and the value of the clear sky noon normal irradiance (Eq.8) [3,4]. The value of I_s, takes into account both diffuse and beam radiation.

$$G_{G_{\lambda i.ext}} = I_s \cdot cos\theta \tag{8}$$

Equation (2) represents the Cauchy's equilibrium equation, of static equilibrium, where σ is the stress tensor formulated following the Hooke's law (Eq.9) and F_v stands for the body forces[5]. The thermal deformations ε_{th} are calculated as presented in Eq. (10).

$$\sigma = \sigma = \boldsymbol{C}\,(E,\nu) : \varepsilon_{el} = \boldsymbol{C}\,(E,\nu) : (\varepsilon - \varepsilon_{th}) \tag{9}$$

$$\varepsilon_{th} = \alpha(T - T_{ref}) \tag{10}$$

Where α is the coefficient of thermal expansion and T_{ref} the strain reference temperature. Thermal deformations can generate stresses in the case of non-uniform temperature fields, or in case the thermal expansions are prohibited from taking place. This

occurs when the materials have different thermal expansion coefficient, as occurs in the presented study, or because of boundary restrictions.

Numerical Model

The numerical model was implemented in COMSOL Multiphysics® software by using the Heat Transfer with Surface-to-Surface Radiation and the Structural Mechanics modules. Two different modeling strategies are here compared. In the first, a *full-domain* approach is adopted. Each component of the strengthened slab is modeled using three-dimensional elements. This means, that the numerical model accurately reproduces the geometry made of three different parts: concrete (5 x 1 x 0.22 m^3), adhesive (5 x 0.1 x 0.002 m^3) and CFRP (5 x 0.1 x 0.0012 m^3). This approach requires a special attention during the meshing phase. In fact, as highlighted in Figure 3, in order to avoid highly distorted elements size a mesh refinement for CFRP and epoxy adhesive need to be implemented. By following a similar approach a high number of mesh elements is required, and the computational time might increase significantly.

In the second, a *lumped boundary approach*, an alternative strategy has been adopted to model the CFRP and adhesive domains. Due to the high geometrical aspect-ratio, CFRP and adhesive can be considered as a thin domain of solids and can be modeled with lumped boundaries instead of full domains. The thin structure domain, i.e. lumped boundary, is represented by the product space between the boundary and the additional dimension for the thickness. In the framework of the heat transfer interface, the calculation of the conductive heat transfer is performed in an extra dimension, representing the thickness of the element. In COMSOL Multiphysics® software the use of a *thin layer* that adopts the general formulation[3], allows the solution of the conductive heat transfer problem into the boundaries (tangential direction) and through the thickness (normal direction) of the structure. Sandwich structure, as for example in the current study CFRP and adhesive can be considered as multiple layers, by assigning to each layer the property of the material. More detail on the theory regarding the heat transfer in thin structures can be found in [3]. By adopting this strategy the geometry is simplified, this facilitates the meshing procedure and the reduction of elements number, lowers the computational time.

The modeling strategy adopted to solve the structural mechanic's problem follows the same path indicated by the previously described thermal step. In the full-domain approach, FRP and adhesive are represented by solid elements and the coupling between thermal and mechanical model has been implemented by providing the output temperature field as input in the structural mechanic so to calculate the thermal stresses in each point of the domain. In the conductive lumped boundary approach both CFRP and adhesive are modeled as layered shell element. The mechanical coupling between solid and shell elements is in this case required; it can be done by using the solid-shell connection feature in the Multiphysics node, or by manually assigning the same variable for the displacement field.

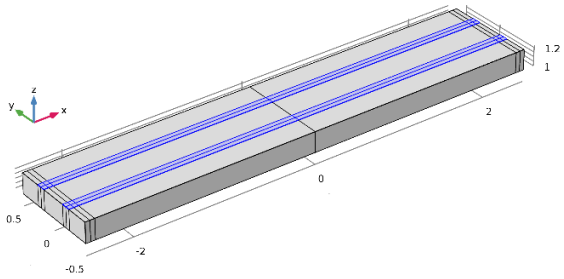

(a)

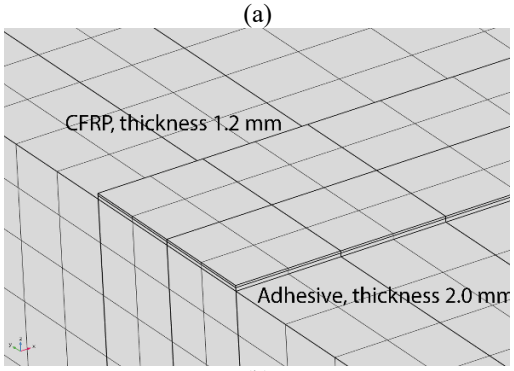

(b)

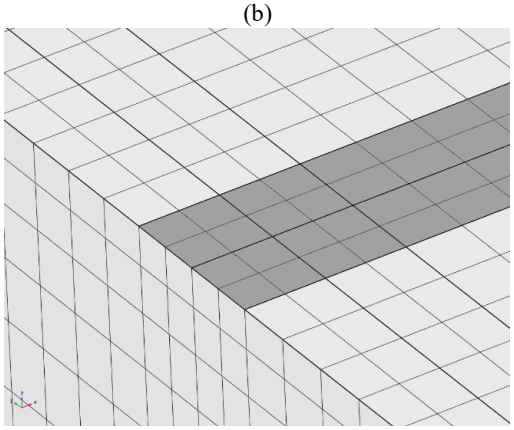

(c)

Figure 3. Difference between the adopted modeling strategies. (a) Geometry of the simulated slab, CFRP strips and adhesive are highlighted in blue (b) Mesh detail of the full-domain approach (c) Mesh detail of the lumped boundary approach (The CFRP-adhesive boundary is highlighted).

The main simplifying assumption in this model lies in the temperature values assumed in the shells elements. In fact, the mapping of the temperature profile along the extra-dimension into the shell thickness is not available. This means that the temperature T used for the calculation of the thermal strain, as indicated in Eq. 10, in the shells elements is equal to the temperature of the concrete boundaries in contact with the adhesive.

Nevertheless, due to the small thickness of adhesive and CFRP, the temperature in the shells can be approximated to the temperature of the concrete boundary without fall into significant errors in the calculation of the CFRP stress. For higher values of thickness this coupling approach might not be recommended, because the thermal bending in the shells might be relevant. Figure 3 shows the difference between the adopted modeling strategies, the position of the CFRP strips, is highlighted (Figure 3a). A swept meshing technique generating regular hexahedra for both models is adopted; this allows a mesh distribution characterized by smaller elements height in the proximity of the top surface. Figure 3b shows the mesh refinement for the full-domain approach, FRP and adhesive are 1.2 and 2 mm thick; a single element has been used for both FRP and adhesive thickness. In Fig 3c, a similar mesh for the lumped boundary approach is shown; the CFRP and adhesive conductive properties are in this case embedded in the boundary layer. Apart from the solid elements used to discretize the adhesive and the CFRP, the mesh are equal for full-domain and lumped boundary approaches. An offset feature is used to take into account the eccentricity between the shells and the solid surface.

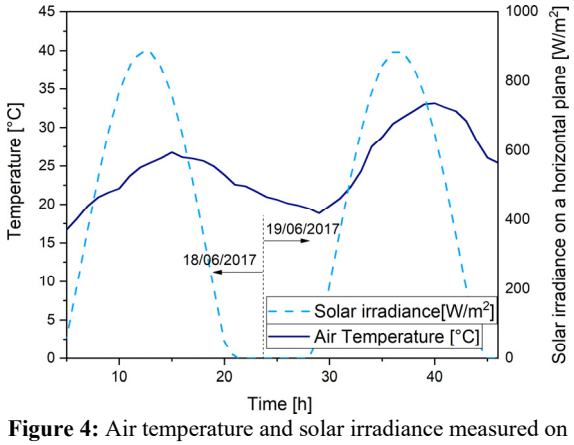

Figure 4: Air temperature and solar irradiance measured on a horizontal plane in Dübendorf (Switzerland) in June 2017 used for the numerical study.

As this is a preliminary study, basic material properties have been used in the simulations. The heat transfer coefficient h is set equal for the entire surface neglecting the face orientation. In a similar way the coefficient of emissivity is assumed equal for concrete and protective paint. The material parameters used in the simulations are shown in Table 1.

Figure 4 shows the values of air temperature and of solar irradiance used for the simulation, and measured in Dübendorf (Switzerland) the 18th and 19th June 2017. The ambient temperature represents the air temperature measured under the slab, and the values of clear sky noon normal irradiance I_s have been obtained from the radiation measurement on a horizontal plane using a silicon-cell pyranometer.

Table 1: Parameters used for the numerical study.

Var.	Value [Units]	Description
$c_{p,conc}$	900 [J/(kgK)]	Heat capacity-concrete
ρ_{conc}	2400 [kg/m^3]	Density-concrete
k_{conc}	1.6 [W/(mK)]	Thermal conductivity-concrete
α_{conc}	10e-6 [1/K]	Thermal expansion concrete
E_{conc}	34e9 [Pa]	E modulus concrete
ν_{conc}	0.2	Poisson coeff.-concrete
$c_{p.adh}$	900 [J/(kgK)]	Heat capacity adhesive
ρ_{adh}	1750[kg/m^3]	Density - adhesive
k_{adh}	5.6[W/(mK)]	Thermal conductivity- adhesive
α_{adh}	5e-5[1/K]	Thermal expansion- adhesive
E_{ach}	7.1[GPa]	E modulus-adhesive
ν_{adh}	0.25	Poisson coeff.-adhesive
c_{pCFRP}	1310[J/(kgK)]	Heat capacity-CFRP
ρ_{CFRP}	1600[kg/m^3]	Density-CFRP
k_{CFRP}	1.3 [W/(mK)]	Thermal conductivity-CFRP
α_{CFRP}	10e-10 [1/K]	Thermal expansion-CFRP
E_{CFRP}	165 [GPa]	E modulus CFRP
ν_{CFRP}	0.1	Poisson CFRP
I_s	973[W/m^2]	Clear sky noon normal irradiance
ε_{b1}	0.65 [--]	Surface emissivity (ambient)
ε_{b2}	0.95 [--]	Surface emissivity (solar)
h	20 [W/(m^{2}K)]	Heat transfer coefficient
T_{ref}	23 [°C]	Reference Temperature

Simulation Results and discussion

The simulation for two consecutive days is here presented. The 18th and 19th June 2017 were selected for this preliminary study because during this days the solar irradiance is typically strong and the sky was clear for the entire measurement period. In the following plots, the starting time is set to the midnight of the 18th June. Figure 5 shows the temperature in the epoxy adhesive, under the CFRP strip that reaches the highest temperature. This temperature is evaluated at a distance of 0.8 m from the support and is compared with the measurement obtained from thermocouple installed in the epoxy. It is possible to notice that the two approaches provide a reasonable estimation of the temperature development over time. Both models reach the peak of temperature at 14:00h (14h) and 15:00h (39h) for the first and second day of simulation.

A slight difference between the models can be observed for the first peak. The lumped-boundary approach is initially closer to the experimental value, however, the difference between the two models is reduced in the afternoon and becomes negligible during the second day of simulation.

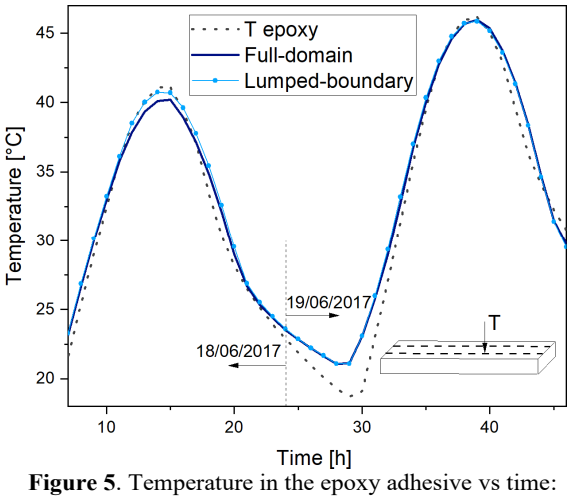

Figure 5. Temperature in the epoxy adhesive vs time: comparison between full-domain approach and lumped boundary approach.

The maximum temperature achieved in the epoxy adhesive is approximately 46°C. In Figure 6, the temperature along the cross-section height (z-coordinate starting from the bottom of the concrete slab) are presented for time-steps equal to 14 and 39 h. The difference of temperature at the bottom surface (z=0.0m) is imperceptible, however, as the top surface is approached differences between the two models arise. A zoom (Figure 6b) on the temperature distribution of the CFRP and adhesive layers provides a better understanding of the differences. It can be noticed that a difference between the two approaches of approximately 0.5°C at the first peak it reduces to ~ 0.25°C at the second day's peak.

The difference between the two models is mainly related to geometrical issues. When the temperature of the concrete surface is plotted along the y-coordinate (slab width) it is possible to find out more about the difference between the full-domain and the lumped boundary approaches. In Figure 7, it can be seen, how, in the full-boundary approach the CFRP-adhesive layers provide a higher insulation at the edge; the temperature of the concrete surface under the adhesive drops more when compared to the superficial temperature calculated using the lumped approach. The temperature on the top surface of the adhesive (full-boundary only) is also shown in Figure 7. Despite the ability of the general formulation in the thin layer to assume the heat transfer in both tangential and normal direction in the lumped boundary approach, it seems that the geometry plays a dominant role.

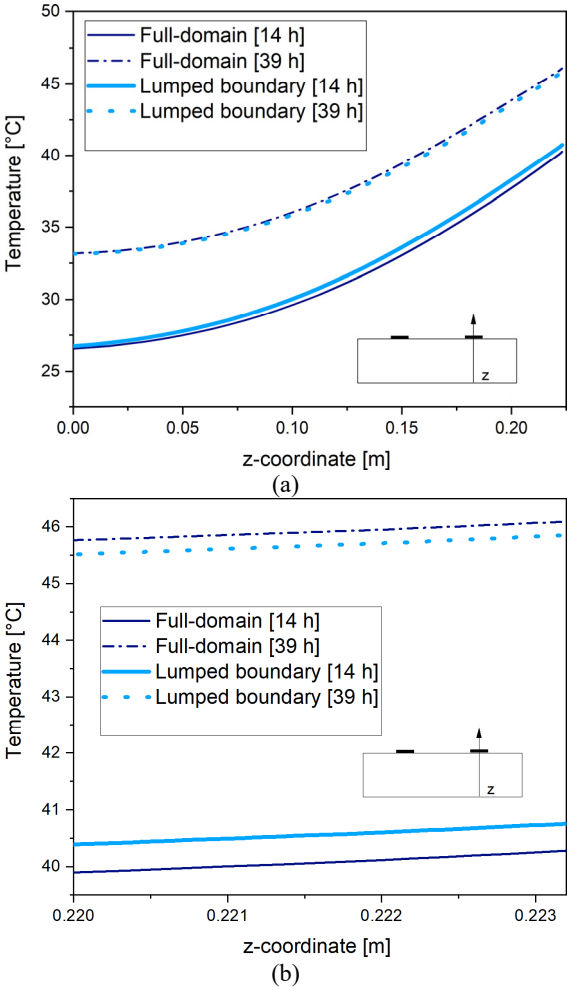

Figure 6. Comparison between full-domain approach and Lumped boundary approach: (a) Total height of the cross section (b) focus on the adhesive and CFRP coordinates. *To plot the temperature in the extra dimension the operator: atxd2([x-cord], [y-cord], [z-cord], ht.tl1.Txdim), been used.*

In the previous section, it was highlighted that in the lumped approach the temperature in the adhesive and CFRP shells for the thermal expansion is the same as the one for the concrete surfaces. In Figure 8 it is shown that this approximation does not significantly affect the thermal stresses in the CFRP strip. In the figure, the longitudinal stress at two different time steps for both modeling strategies is shown. The main difference of stress at h=14 it might be directly related by the higher temperature calculated with the lumped-boundary approach as discussed for Figure 5.

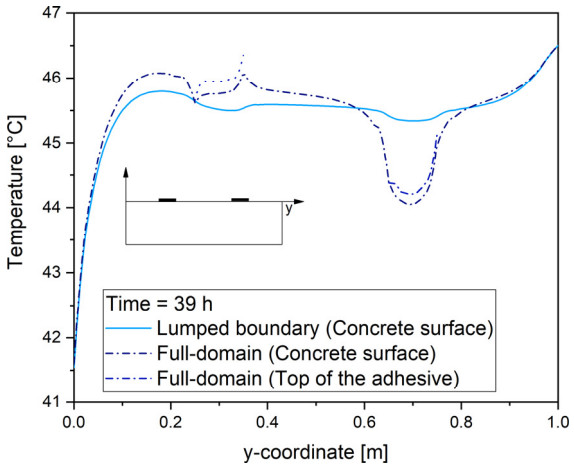

Figure 7. Temperature on the top surface of the concrete slab width.

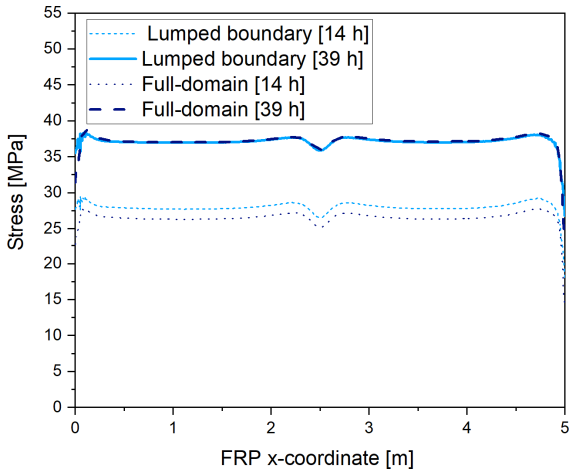

Figure 8. CFRP stress vs FRP x-coordinate.

The longitudinal stress in the CFRP stips, due to the slab thermal expansion is almost constant for the entire length (x-coordinate), with the only exception of the strips end, where, as expected, it drops to zero (Figure 8). This implies that the shear stress at the CFRP concrete interface, typically evaluated as the change of force in the FRP divided by the contact area, presents a peak of stress at the strip-end which rapidly decreases to zero, as the distance from the end increases. The value of the peak stress and affected length are not discussed in this paper. Nevertheless, these results show how the end anchorage section is affected by the thermal deformation, and where the bond interface can be mainly affected. Figure 9 shows the CFRP stress vs time for one strip. No relevant difference between the modeling strategies can be observed. The values of CFRP stress fluctuate between 0 and 37 MPa. The calculated longitudinal stress range can be considered relatively low when compared to the design debonding stress. In a similar way, the shear stress generated at the interface does not significantly affect the bond strength of the stip-end anchorage. However further studies are necessary to evaluate if a stress ranges of this entity can reduce the life of the strengthening and lead to premature debonding when service loads and critical environmental conditions are taken into account.

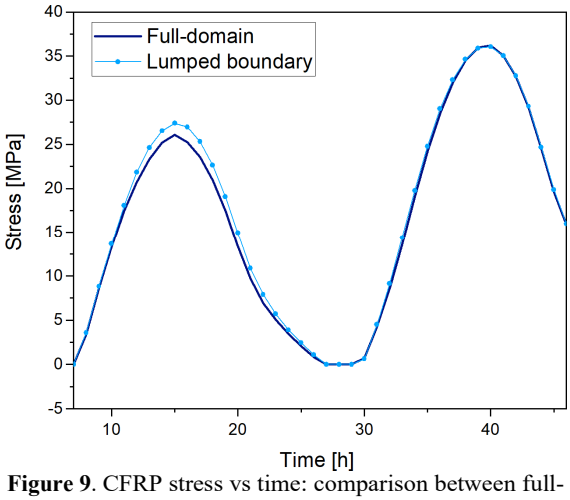

Figure 9. CFRP stress vs time: comparison between full-domain approach and lumped boundary approach.

Conclusions

A strengthening application for RC decks of road bridges has been studied in this paper; the effects of the high environmental temperature and solar radiation on CFRP strips bonded on the concrete surface are considered. In order to evaluate the temperature along the cross-section and the thermally-induced stresses in the CFRP strip, two different modeling approaches have been compared: the full-domain approach and the boundary layer approach.It was observed that both models can fit the experimental measurements. For the simulated time-frame, the temperature of the adhesive reached an approximate value of 46°C, which corresponds approximately to a 13°C higher value than the maximum measured air temperature. It has also been shown that the stress in the FRP generated by the change of daily temperature is negligible in comparison to the one typically generated from external loads.

It can be concluded that the full-domain approach can provide more accurate and detailed results, however, the required computational time is higher. For the discussed problem, fairly accurate results can be obtained with the boundary layer approach, for both thermal and mechanical problems. By using this latter approach the computational time can be also reduced.

The high temperature reached in the epoxy adhesive can lead to the loss of bond between the FRP and the concrete surface. This outcome implies that when the CFRP strengthening faces directly the solar radiation, an additional protective layer or higher safety factors might be necessary. Further studies are needed to evaluate if the thermally generated stresses combined with sustained loads in high- temperature environments can affect the long-term behavior of bonded CFRP strengthening.

References

1. Michels J., Widmann R., Czaderski C., Allahvirdizadeh R., Motavalli M. Glass transition evaluation of commercially available epoxy resins used for civil engineering applications. Composites Part B: Engineering, **77**, 484-493, (2015).

2. Gallego J. M., Michels J., Czaderski C. Influence of the asphalt pavement on the short-term static strength and long-term behaviour of RC slabs strengthened with externally bonded CFRP strips. Engineering Structures, **150**, 481-496, (2017).

3. Heat Transfer Module User's Guide 5.3, COMSOL, Inc, www.comsol.com

4. Duffie, J.A., Beckmann, W.A. Solar Engineering of Thermal Processes, 936 pages, John Wiley&Sons, Inc. (4 edition, 2013).

5. Structural Mechanics Module User's Guide, 5.3, COMSOL, Inc, www.comsol.com

Acknowledgments

The authors want to acknowledge the financial support of the Federal Road Office – FEDRO (Astra Projects Nos. AGB:2012/001, AGB:2016/003).